

Journal of Electrochemistry

Volume 19

Issue 3 Special Issue of Lithium-Ion Batteries
and Fuel Cells (Editor: Professor DONG Quan-
feng)

2013-06-28

Fabrication and Performance of $\text{LaNi}_{0.6}\text{Fe}_{0.4}\text{O}_3-\gamma'$ Cathode Modified by Coating with $\text{Gd}_{0.2}\text{Ce}_{0.8}\text{O}_2$ for Intermediate Temperature Solid Oxide Fuel Cell

Rui-xuan REN

Bo HUANG

Xin-jian ZHU

Yi-xing Hu

Xiao-yi DING

Zong-yao LIU

Ye-bin LIU

Recommended Citation

Rui-xuan REN, Bo HUANG, Xin-jian ZHU, Yi-xing Hu, Xiao-yi DING, Zong-yao LIU, Ye-bin LIU. Fabrication and Performance of $\text{LaNi}_{0.6}\text{Fe}_{0.4}\text{O}_3-\gamma'$ Cathode Modified by Coating with $\text{Gd}_{0.2}\text{Ce}_{0.8}\text{O}_2$ for Intermediate Temperature Solid Oxide Fuel Cell[J]. *Journal of Electrochemistry*, 2013 , 19(3): Article 13.

DOI: 10.61558/2993-074X.2960

Available at: <https://jelectrochem.xmu.edu.cn/journal/vol19/iss3/13>

This Article is brought to you for free and open access by Journal of Electrochemistry. It has been accepted for inclusion in Journal of Electrochemistry by an authorized editor of Journal of Electrochemistry.

文章编号:1006-3471(2013)03-0275-06

Gd_{0.2}Ce_{0.8}O₂包覆LaNi_{0.6}Fe_{0.4}O_{3-δ}阴极制备及性能

任睿轩, 黄波*, 朱新坚, 胡一星, 丁小益, 刘宗尧, 刘烨彬

(上海交通大学 机械与动力工程学院, 燃料电池研究所, 上海 200240)

摘要: 应用丝网印刷和共烧结法制备 LaNi_{0.6}Fe_{0.4}O_{3-δ}/Sc_{0.1}Zr_{0.9}O_{1.95}/LaNi_{0.6}Fe_{0.4}O_{3-δ} 对称电池。以硝酸铈和硝酸钆为原料, 柠檬酸作燃料, 燃烧合成 Gd_{0.2}Ce_{0.8}O₂(GDC)包覆的 LaNi_{0.6}Fe_{0.4}O_{3-δ} (LNF)阴极。实验表明, 在 750 °C 工作温度下, 纯 LaNi_{0.6}Fe_{0.4}O_{3-δ} 阴极的极化电阻为 0.70 Ω·cm², 而 21.3% (by mass, 下同, 如无特殊标注均为质量分数)GDC 包覆的 LNF-GDC 复合阴极的极化电阻最小(0.13 Ω·cm²), 活化能最低(136.80 kJ·mol⁻¹), 故其阴极性能最佳。GDC 的包覆加速了气体/阴极/电解质三相界面反应区的扩散过程, 降低了阴极极化电阻。

关键词: 固体氧化物燃料电池; LaNi_{0.6}Fe_{0.4}O_{3-δ} 阴极; Gd_{0.2}Ce_{0.8}O₂ 包覆; 极化电阻; 交流阻抗

中图分类号: TM911

文献标识码: A

在固体氧化物燃料电池 (Solid Oxide Fuel Cell, SOFC) 的发展过程中, 人们越来越认识到降低电池工作温度的重要性。若能将电池工作温度降低到中温 (600 ~ 800 °C), 则能提高电极的稳定性, 减小热应力, 延长电池寿命, 还可使用廉价的金属合金作为电池的双极板材料^[1-3]。Cr 基合金因具有成本低、易加工、电子电导率和热导率高、机械稳定性高、耐高温以及抗氧化等优点而成为最有前景的双极板材料^[4-6]。Cr 基合金用于 SOFC 的双极板时, 高价态 Cr 化合物易挥发, 而低导电性的 Cr₂O₃(s) 在阴极/电解质界面的生成与聚集又会降低 SOFC 的电输出性能^[7-10], 且 CrO₃(g) 和 Cr₂O₃(s) 可与阴极材料如 (La,Sr)MnO₃ 反应生成绝缘的尖晶石相 (Cr,Mn)₃O₄(s), 即发生阴极“Cr 中毒”现象^[11], 使电池性能急剧下降。

据 Chiba 等^[12]报道, LaNi_{0.6}Fe_{0.4}O_{3-δ}(LNF) 800 °C 电导率为 580 S·cm, 为传统阴极 La_{0.8}Sr_{0.2}MnO₃(LSM) (180 S·cm) 的 3 倍, 其室温 ~ 1000 °C 热膨胀系数为 11.4 × 10⁻⁶ K⁻¹, 更接近于电解质 YSZ(Yttria Stabilized Zirconia, Y_{0.08}Zr_{0.92}O_{1.95}) 的热膨胀系数 10.0 × 10⁻⁶ K⁻¹。Zhen 等^[13]研究也表明 LNF 比 LSM 具有更稳定的电化学性能, Fe-Cr 合金存在时, 其界面上没有 Cr 沉积, LNF 有抗 Cr 毒化作用。然在相同的烧结温度 LNF 较 LSM 更易与 ZrO₂ 基电解质反应^[14-15], 如高于 1000 °C 时 LNF 与 ZrO₂ 基电解质反应生成

绝缘的 La₂Zr₂O₇, 降低电池性能。由于 LNF 阴极材料在工作温度下的再氧化以及随后的氧空位浓度的下降^[16], 致使 LNF 阴极的初始性能下降。Stodolny 等^[17-18]研究发现, 由于 CrO₃(g) 或 CrO₂(OH)₂(g) 等挥发性的物质与阴极 LaNi_{0.6}Fe_{0.4}O_{3-δ} 发生反应而使其欧姆电阻和极化电阻增加。本文应用燃烧合成法, 在已烧结的 LNF 阴极表面包覆一层 Gd_{0.2}Ce_{0.8}O₂(GDC) 纳米颗粒制成 LNF-GDC 复合阴极, 该阴极的导电性降低不显著, 可阻止 LNF 与电解质 ScSZ(Scandia Stabilized Zirconia, Sc_{0.1}Zr_{0.9}O_{1.95}) 生成绝缘的 La₂Zr₂O₇, 以期增大阴极材料-电解质材料-反应气体三相界面, 改善 LNF 阴极性能。

1 实验

1.1 LNF-GDC 复合阴极的制备

按 La:Ni:Fe = 1:0.6:0.4(by mole) 称取一定量的 La(NO₃)₃·6H₂O、Ni(NO₃)₂ 和 Fe(NO₃)₃·9H₂O 配成混合溶液, 加入一定比例的柠檬酸(柠檬酸与硝酸盐的化学配比计算方法参见文献^[19]), 用氨水将混合液调至中性, 将其 120 °C 加热蒸发, 得褐色干凝胶, 置于坩埚电炉(300 °C 预热)燃烧, 升温至 600 °C 烧烧 2 h 可得黑色 LaNi_{0.6}Fe_{0.4}O_{3-δ} (LNF) 粉体材料。详细的粉体制备方法参见文献^[20]。

将 LNF 阴极浆料通过丝网印刷覆盖于 ScSZ 片(厚约 200 μm)两侧, 1050 °C 烧烧 2 h 印制成

LNF/ScSZ/LNF 对称电池 (面积为 $1\text{ cm} \times 1\text{ cm} = 1\text{ cm}^2$).

GDC 溶液(见文献^[21]):按 Gd:Ce = 1:4(by mole) 取一定量的 $\text{Gd}(\text{NO}_3)_3 \cdot 6\text{H}_2\text{O}$ 和 $\text{Ce}(\text{NO}_3)_3 \cdot 6\text{H}_2\text{O}$ 与一定化学计量比的柠檬酸溶于蒸馏水中, 配制成 Gd^{3+} 浓度为 $0.4\text{ mol} \cdot \text{L}^{-1}$ 的溶液. 将上述 LNF 阴极浸入此溶液, 在低于 200 MPa 真空度下保持 30 min, 使溶液充分浸润 LNF, 又将其移置于烘箱 75°C 烘干, 移入预热至 450°C 的坩埚电炉内即升温至 600°C , 保温 2 h. 按上述步骤重复数次, 即得 $\text{Gd}_{0.2}\text{Ce}_{0.8}\text{O}_2$ (GDC)($\leq 50\text{ nm}$) 包覆的 LNF 对称电池, 铂网为电流收集体.

1.2 LNF-GDC 复合阴极的表征

采用阿基米德排水法测试 GDC 包覆的 LNF 阴极样品的孔隙率, 使用 Solartron 1260 阻抗仪测试电池交流阻抗(开路), 测试频率 $10\text{ mHz} \sim 100\text{ kHz}$, 交流阻抗输入信号 20 mV , 工作温度: 650°C 、 700°C 、 750°C 、 800°C 和 850°C . 使用扫描电子显微镜(SEM, PHILIPS 515 型)观察材料微观形貌.

2 结果与讨论

2.1 LNF-GDC 复合阴极表征

表 1 给出不同 GDC 包覆量的 LNF-GDC 复合阴极的孔隙率. 可以看出, 纯 LNF 阴极的孔隙率为 38.1%, 经 1 次包覆后, 其孔隙率为 32.2%, GDC 包覆量为 4.7% (5.9%, by volume). 包覆次数增加, GDC 包覆量也逐渐递增, 其阴极孔隙率降低. 经 6 次包覆 GDC, 其阴极孔隙率降为 0.05%.

表 1 不同 GDC 包覆量的 LNF-GDC 复合阴极的孔隙率参数
Tab. 1 Porosity and GDC loading of the impregnated LNF cathode

Coating cycle	0	1	2	4	5	6
Porosity/%	38.1	32.2	24.6	13.1	6.2	0.05
Loading/% (by mass)	0	4.7	8.1	15.9	21.3	26.9
Loading/% (by volume)	0	5.9	13.5	25.0	31.9	38.1

图 1 示出 21.3% (A) 和 26.9% (B) GDC 包覆量的 LNF-GDC 复合阴极的 SEM 照片. 可以看出, 包覆量 21.3% 时, GDC 颗粒覆盖于 LNF 颗粒表面, 彼此联通, 形成网络. 包覆量增至 26.9% 时, GDC 颗粒堵塞阴极气孔, 使阴极孔隙率下降.

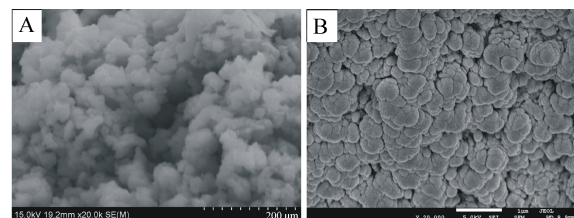


图 1 21.3% (A) 和 26.9% (B) GDC 包覆量的 LNF-GDC 复合阴极的 SEM 照片

Fig. 1 SEM images of 21.3% (A) and 26.9% (B) GDC-impregnated LNF-GDC composite cathodes

2.2 LNF-GDC 复合阴极电化学性能

图 2 给出不同 GDC 包覆量的 LNF-GDC 复合阴极分别在 750°C (A) 和 800°C (B) 工作温度下的交流阻抗谱图和等效电路图(C). 由图可知, 该阻抗谱图是由高频弧和低频弧组成. 其高频弧对应于阴极/电解质界面的电化学反应过程(界面极化电阻或电荷传递电阻 R_{ct}), 低频弧对应于气体扩散过程(浓差极化电阻 R_d), 阴极极化电阻 $R_p = R_{ct} + R_d$ ^[22-25], R_Ω 为对称电池的欧姆电阻. 随 GDC 包覆量增加, 其阴极的电荷传递电阻 R_{ct} 变化甚微, 而浓差极化电阻 R_d 渐减, 欧姆电阻 R_Ω 几乎不变. 包覆量增至 26.9%, 欧姆电阻 R_Ω 显著增加, 阴极浓差极化电阻 R_d 也递增. 650°C 、 700°C 以及 850°C 工作温度下阴极的交流阻抗谱图具有同样的趋势.

图 3 和图 4 分别给出不同工作温度下 GDC 包覆量与对称电池的欧姆电阻 R_Ω 和阴极极化电阻 R_p 的关系图. 由图发现, 同工作温度下 GDC 包覆量由 0 增至 21.3%, 其对称电池的欧姆电阻几乎不变, 而阴极极化电阻逐渐降低. 显然, GDC 包覆极大地改善了该电极的电化学性能, GDC 的存在加速气体/阴极/电解质三相界面反应区的扩散过程, 降低阴极极化电阻^[26]. GDC 包覆量为 21.3% 的 LNF-GDC 复合阴极, 其极化电阻最低, 在 850°C 、 800°C 、 750°C 、 700°C 和 650°C 工作温度其值分别为 $0.03\text{ } \Omega \cdot \text{cm}^2$ 、 $0.06\text{ } \Omega \cdot \text{cm}^2$ 、 $0.13\text{ } \Omega \cdot \text{cm}^2$ 、 $0.29\text{ } \Omega \cdot \text{cm}^2$ 和 $1.47\text{ } \Omega \cdot \text{cm}^2$; 而纯 LNF 阴极的极化电阻在相应工作温度下分别为 $0.12\text{ } \Omega \cdot \text{cm}^2$ 、 $0.28\text{ } \Omega \cdot \text{cm}^2$ 、 $0.70\text{ } \Omega \cdot \text{cm}^2$ 、 $1.91\text{ } \Omega \cdot \text{cm}^2$ 和 $5.62\text{ } \Omega \cdot \text{cm}^2$. 750°C 时, GDC 包覆量为 21.3% 的 LNF-GDC 复合阴极的极化电阻($0.13\text{ } \Omega \cdot \text{cm}^2$)比纯 LNF 阴极的极化电阻($0.70\text{ } \Omega \cdot \text{cm}^2$)降低了大约 4 倍. 但当包覆量增至 26.9% 时, 其欧姆电阻急剧增加, 阴极极化电阻亦

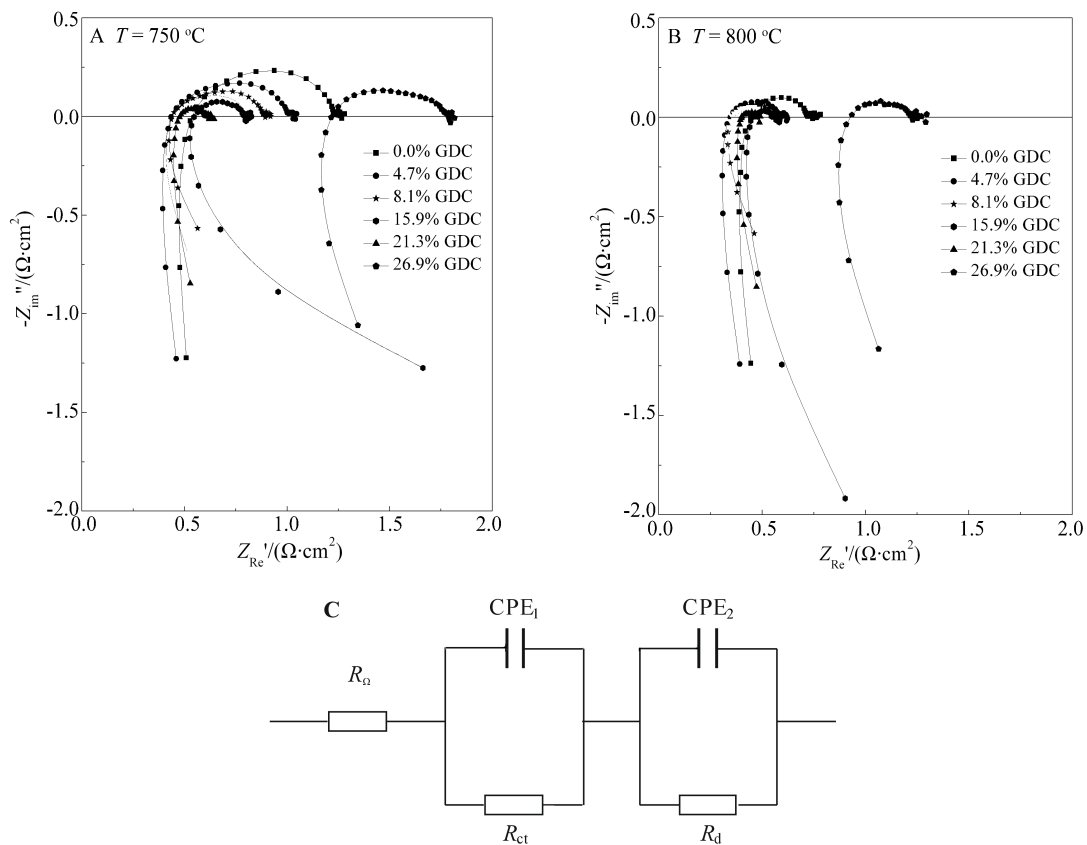


图 2 不同 GDC 包覆量的 LNF-GDC 复合阴极在工作温度 750 °C(A)和 800 °C(B)的电化学阻抗谱图及等效电路图(C)

Fig. 2 Electrochemical impedance spectra of the LNF-GDC composite cathode with different contents of GDC measured at 750 °C(A), 800 °C (B) in air and the equivalent circuit for data fitting (C)

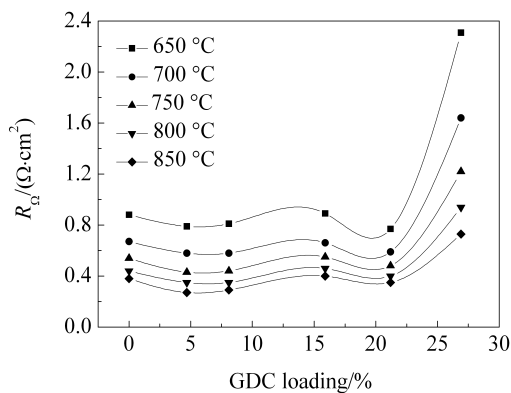


图 3 不同温度下测得对称电池欧姆电阻与 GDC 包覆量变化的示意图

Fig. 3 Plots of ohmic resistance of symmetrical cell versus the contents of GDC obtained at different temperatures

增加。这是因为, GDC 是氧离子导体, 26.9% GDC 包覆的 LNF-GDC 复合阴极的孔隙率接近于 0, 导致欧姆电阻增加、气相传输过程减弱和浓差极化增

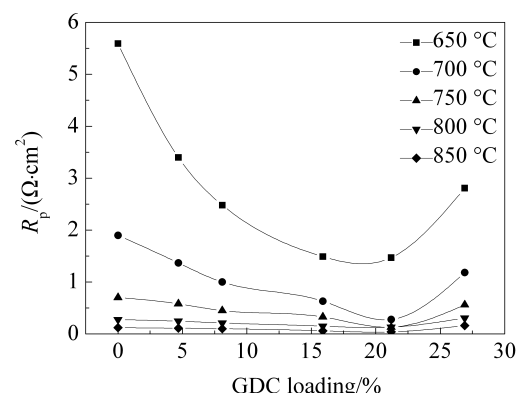


图 4 不同温度下测得对称电池阴极极化电阻与 GDC 包覆量变化的示意图

Fig. 4 Plots of polarization resistance of LNF-GDC composite cathodes versus the contents of GDC obtained at different temperatures

加。GDC 包覆量 21.3% 的 LNF-GDC 复合阴极有最低的阴极极化电阻值, 这源于离子导体和电子导体达到适当的比率。

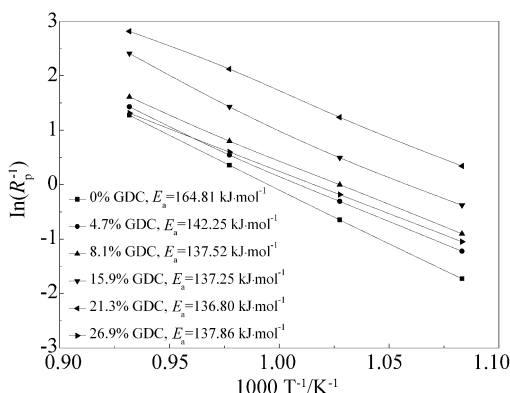


图 5 不同 GDC 包覆量 LNF-GDC 复合阴极的阿伦尼乌斯曲线

Fig. 5 Arrhenius curves of LNF-GDC composite cathodes with different contents of GDC

图 5 给出不同 GDC 包覆量的 LNF-GDC 复合阴极的阿伦尼乌斯曲线, 据式:

$$\frac{1}{R_p} = A \cdot \exp\left(-\frac{E_a}{kT}\right) \quad (1)$$

其中, A 为常数, k 为波尔兹曼常数, E_a 为活化能, R_p 为极化电阻。从阿伦尼乌斯曲线斜率可得活化能, 纯 LNF 阴极的活化能为 $164.81 \text{ kJ} \cdot \text{mol}^{-1}$, 4.7% GDC、8.1% GDC、15.9% GDC、21.3% GDC、26.9% GDC 包覆的 LNF 复合阴极的活化能分别为 $142.25 \text{ kJ} \cdot \text{mol}^{-1}$ 、 $137.52 \text{ kJ} \cdot \text{mol}^{-1}$ 、 $137.25 \text{ kJ} \cdot \text{mol}^{-1}$ 、 $136.80 \text{ kJ} \cdot \text{mol}^{-1}$ 和 $137.86 \text{ kJ} \cdot \text{mol}^{-1}$ 。其中 21.3% GDC 包覆的 LNF-GDC 复合阴极的活化能最小, 其性能最佳。

3 结 论

由燃烧合成法在已烧结的 LNF 阴极表面包覆 GDC 制成的 LNF-GDC 复合阴极, 随 GDC 包覆量 ($\leq 21.3\%$) 增加, 其欧姆电阻几乎不变, 极化电阻显著减小; 21.3% GDC 包覆其颗粒相互接触形成联通网络, 而 GDC 包覆量增至 26.9% 其颗粒堵塞阴极气孔, 欧姆电阻显著增加。21.3% GDC 包覆的 LNF-GDC 复合阴极性能最佳。在 850°C 、 800°C 、 750°C 、 700°C 和 650°C 工作温度其极化电阻分别为 $0.03 \Omega \cdot \text{cm}^2$ 、 $0.06 \Omega \cdot \text{cm}^2$ 、 $0.13 \Omega \cdot \text{cm}^2$ 、 $0.29 \Omega \cdot \text{cm}^2$ 和 $1.47 \Omega \cdot \text{cm}^2$, 纯 LNF 阴极的极化电阻分别为 $0.12 \Omega \cdot \text{cm}^2$ 、 $0.28 \Omega \cdot \text{cm}^2$ 、 $0.70 \Omega \cdot \text{cm}^2$ 、 $1.91 \Omega \cdot \text{cm}^2$ 和 $5.62 \Omega \cdot \text{cm}^2$ 。 750°C 工作温度时, 21.3% GDC 包覆量的 LNF-GDC 复合阴极极化电阻较纯 LNF 阴极的极化电阻降低约 4 倍, 其活化能为 $136.80 \text{ kJ} \cdot \text{mol}^{-1}$, 阴极电化学性能最佳。

参 考 文 献(References):

- [1] Lv S Q(吕世权), Long G H(龙国徽), Meng X W(孟祥伟), et al. Perovskite cathode for solid oxide fuel cells[J]. Chinese Journal of Power Source (电源技术), 2010, 34(7): 734-737.
- [2] Guo Y B(郭友斌), Lu L H(陆丽华), Chu L(储凌), et al. Research progress in perovskite-like cathode for intermediate temperature solid oxide fuel cells[J]. Bulletin of the Chinese Ceramic Society(硅酸盐通报), 2009, 28(5): 991-996.
- [3] Wu L W(邬理伟), Zheng Y P(郑颖平), Sun Y M(孙岳明), et al. Research progress in composite cathode of SOFC[J]. Chinese Battery Industry(电池工业), 2010, 15(1): 53-56.
- [4] Kadowaki T, Shiomitsu T, Marsuda E, et al. Applicability of heat resisting alloys to the separator of planar type solid oxide fuel cell[J]. Solid State Ionics, 1993, 67(1/2): 65-69.
- [5] Yang Z, Weil K S, Paxton D M, et al. Selection and evaluation of heat-resistant alloys for SOFC interconnect applications[J]. Journal of the Electrochemical Society, 2003, 150(9): A1188-A1201.
- [6] Horita T, Xiong Y, Kishimoto H, et al. Application of Fe-Cr alloys to solid oxide fuel cells for cost-reduction: Oxidation behavior of alloys in methane fuel[J]. Journal of Power Sources, 2004, 131(1/2): 293-298.
- [7] Tucker M C, Kurokawa H, Jacobson C P, et al. A fundamental study of chromium deposition on solid oxide fuel cell cathode materials[J]. Journal of Power Sources, 2006, 160(1): 130-138.
- [8] Konysheva E, Penkalla H, Wessel E, et al. Chromium poisoning of perovskite cathodes by the ODS alloy Cr₅Fe₁Y₂O₃ and the high chromium ferritic steel Crofer22APU[J]. Journal of the Electrochemical Society, 2006, 153(4): A765-A773.
- [9] Yokokawa H, Horita T, Sakai N, et al. Thermodynamic considerations on Cr poisoning in SOFC cathodes[J]. Solid State Ionics, 2006, 177(35/36): 3193-3198.
- [10] Liu D J, Almer J, Cruse T. Characterization of Cr poisoning in a solid oxide fuel cell cathode using a high energy X-ray microbeam [J]. Journal of the Electrochemical Society, 2010, 157(5): B744-B750.
- [11] Horita T, Xiong Y P, Kishimoto H, et al. Chromium poisoning and degradation at (La,Sr)MnO₃ and (La,Sr)FeO₃ cathodes for solid oxide fuel cells[J]. Journal of the Electrochemical Society, 2010, 157(5): B614-B620.
- [12] Chiba R, Yoshimura F, Sakurai Y. An investigation of

- $\text{LaNi}_{1-x}\text{Fe}_x\text{O}_3$ as a cathode material for solid oxide fuel cells[J]. Solid State Ionics, 1999, 124(3/4): 281-288.
- [13] Zhen Y D, Tok A I Y, Jiang S P, et al. $\text{La}(\text{Ni}_x\text{Fe})\text{O}_3$ as a cathode material with high tolerance to chromium poisoning for solid oxide fuel cells[J]. Journal of Power Sources, 2007, 170(1): 61-66.
- [14] Orui H, Watanabe K, Chiba R, et al. Application of $\text{LaNi}(\text{Fe})\text{O}_3$ as SOFC cathode[J]. Journal of the Electrochemical Society, 2004, 151(9): A1412-A1417.
- [15] Bevilacqua M, Montini T, Tavagnacco C, et al. Preparation, characterization, and electrochemical properties of pure and composite $\text{LaNi}_{0.6}\text{Fe}_{0.4}\text{O}_3$ -based cathodes for IT-SOFC[J]. Chemistry of Materials, 2007, 19: 5926-5936.
- [16] Hashimoto S I, Kammer K, Larsen P H, et al. A study of $\text{Pr}_{0.7}\text{Sr}_{0.3}\text{Fe}_{1-x}\text{Ni}_x\text{O}_{3-\delta}$ as a cathode material for SOFCs with intermediate operating temperature[J]. Solid State Ionics, 2005, 176:1013-1020.
- [17] Stodolny M K, Boukamp B A, Blank D H A, et al. Impact of Cr-poisoning on the conductivity of $\text{LaNi}_{0.6}\text{Fe}_{0.4}\text{O}_3$ [J]. Journal of Power Sources, 2011(22), 196: 9290-9298.
- [18] Stodolny M K, Boukamp B A, Blank D H A, et al. Cr-poisoning of a $\text{LaNi}_{0.6}\text{Fe}_{0.4}\text{O}_3$ cathode under current load[J]. Journal of Power Sources, 2012, 209: 120-129.
- [19] Jain S R, Adiga K C, Vemeker V R P. A new approach to thermochemical calculation of condensed fuel-oxidizer mixtures[J]. Combustion and Flame, 1981, 40(1): 71-76.
- [20] Liu H(刘珩), Huang B(黄波), Zhu X J(朱新坚). Preparation and characterization of the $\text{LaNi}_{0.6}\text{Fe}_{0.4}\text{O}_{3-\delta}$ cathode for intermediate temperature solid oxide fuel cell [J]. Journal of Electrochemistry(电化学), 2011, 17(4): 421-426.
- [21] Huang B, Ye X F, Wang S R, et al. Performance of Ni/ScSZ cermet anode modified by coating with $\text{Gd}_{0.2}\text{Ce}_{0.8}\text{O}_2$ for a SOFC running on methane fuel[J]. Journal of Power Sources, 2006, 162(2): 1172-1181.
- [22] Zhou W, Ran R, Shao Z P, et al. Electrochemical performance of silver-modified $\text{Ba}_{0.5}\text{Sr}_{0.5}\text{Co}_{0.8}\text{Fe}_{0.2}\text{O}_{3-\delta}$ cathodes prepared via electrodes deposition[J]. Electrochimica Acta, 2008, 53(13): 4370-4380.
- [23] Adler S B. Limitations of charge-transfer models for mixed-conducting oxygen electrodes [J]. Solid State Ionics, 2000, 135: 603-612.
- [24] Fu C J, Sun K N, Zhang N, et al. Electrochemical characteristics of LSCF-GDC composite cathodes for intermediate temperature SOFC[J]. Electrochimica Acta, 2007, 52(13): 4589-4594.
- [25] Qiang F, Sun K N, Zhang N Q, et al. Characterization of electrical properties of GDC doped A-site deficient LSCF based composite cathode using impedance spectroscopy[J]. Journal of Power Sources, 2007, 168: 338-345.
- [26] Jiang S P, Leng Y J, Chan S H, et al. Development of $(\text{La},\text{Sr})\text{MnO}_3$ -based cathodes for intermediate temperature solid oxide fuel cells[J]. Electrochemical and Solid-State Letters, 2003, 6(4): A67-A70.
- [27] Li J L, Wang S R, Wang Z R, et al. $(\text{La}_{0.74}\text{Bi}_{0.10}\text{Sr}_{0.16})\text{MnO}_{3-\delta}\text{Ce}_{0.8}\text{Gd}_{0.2}\text{O}_{2-\delta}$ cathodes fabricated by ion-impregnating method for intermediate-temperature solid oxide fuel cells[J]. Journal of Power Sources, 2009, 188(2): 453-457.

Fabrication and Performance of $\text{LaNi}_{0.6}\text{Fe}_{0.4}\text{O}_{3-\delta}$ Cathode Modified by Coating with $\text{Gd}_{0.2}\text{Ce}_{0.8}\text{O}_2$ for Intermediate Temperature Solid Oxide Fuel Cell

REN Rui-xuan, HUANG Bo*, ZHU Xin-jian, HU Yi-xing, DING Xiao-yi,
LIU Zong-yao, LIU Ye-bin

(Institute of Fuel Cell, School of Mechanical Engineering, Shanghai Jiaotong University,
Shanghai 200240, China)

Abstract: The symmetric cell of $\text{LaNi}_{0.6}\text{Fe}_{0.4}\text{O}_{3-\delta}/\text{Sc}_{0.1}\text{Zr}_{0.9}\text{O}_{1.95}/\text{LaNi}_{0.6}\text{Fe}_{0.4}\text{O}_{3-\delta}$ was fabricated with screen printing method. A $\text{LaNi}_{0.6}\text{Fe}_{0.4}\text{O}_{3-\delta}$ (LNF) cathode was modified by coating with nano-sized gadolinium-doped ceria (GDC, $\text{Gd}_{0.2}\text{Ce}_{0.8}\text{O}_2$) prepared using a simple combustion process within the pores of the cathode. According to the electrochemical impedance spectra (EIS), the polarization resistance of the pure LNF was $0.70 \Omega \cdot \text{cm}^2$ at 750°C , while $0.13 \Omega \cdot \text{cm}^2$ for the 21.3%GDC (by mass)-coated LNF cathode at the same temperature, which was only 1/5 of that of the pure LNF cathode. The activation energy of the 21.3% GDC (by mass)-coated LNF cathode ($136.80 \text{ kJ} \cdot \text{mol}^{-1}$) is the smallest among those of GDC-coated LNF cathodes with different contents of GDC. The 21.3% GDC (by mass)-coated LNF cathode showed the optimum performance. The results indicated that GDC coatings significantly affected electrocatalytic activity of the LNF cathodes towards O_2 reduction reaction. The improved performance of GDC-coated LNF cathode was attributed to the extended triple-phase boundary (TPB) and enhanced ion conductivity of oxide.

Key words: solid oxide fuel cell; $\text{LaNi}_{0.6}\text{Fe}_{0.4}\text{O}_{3-\delta}$ cathode; $\text{Gd}_{0.2}\text{Ce}_{0.8}\text{O}_2$ coating; polarization resistance; electrochemical impedance spectroscopy